Available online at www.eccomasproceedia.org
Eccomas Proceedia COMPDYN (2025) 5590-5599

ECCOMAS
Proceedia

COMPDYN 2025
10th ECCOMAS Thematic Conference on
Computational Methods in Structural Dynamics and Earthquake Engineering
M. Papadrakakis, M. Fragiadakis (eds.)
Rhodes Island, Greece, 15-18 June 2025

EFFECTS DUE TO CONCRETE CONFINEMENT ON THE SEISMIC RELIABILITY OF RC FRAMES

Diego Gino[1], **Gabriele Neri**[1], **Gaetano Alfano**[1]

[1] Politecnico di Torino
Corso Duca degli Abruzzi 24, 10129, Turin, Italy
{diego.gino , gabriele_neri, gateano.alfano}@polito.it

Abstract

This study investigates the effects of concrete confinement in the seismic design of reinforced concrete (RC) frames. Current seismic codes rely on capacity design principles, where overstrength is primarily based on the inelastic behavior of reinforcing steel, neglecting the non-linear properties of concrete. However, confinement provided by stirrups and compression can enhance the strength and ductility of concrete during seismic events. In this research, RC frames designed for a high-ductility class in L'Aquila are analyzed, investigating the confinement effects in the different structural elements (i.e., beam, columns and beam-column nodes). Material uncertainties in steel and concrete properties are incorporated using Latin Hypercube Sampling. Incremental dynamic analyses (IDAs) are conducted to derive seismic fragility curves and assess structural reliability according to a performance-based earthquake engineering (PBEE) approach. The results show that current code provisions do not provide adequate safety levels, highlighting the need for improved design methodologies.

Keywords: Seismic reliability, overstrength factor, material uncertainty, reinforced concrete frames, incremental dynamic analysis.

ISSN:2623-3347
Peer-review under responsibility of the organizing committee of COMPDYN 2025.
doi: 10.7712/120125.128 5.24741

1 INTRODUCTION

In recent decades, increasing attention has been given to the structural reliability to enhance the seismic performance of both new and existing reinforced concrete (RC) structures [1]-[6]. To achieve this, the scientific community has developed sophisticated structural models able to capture key post-elastic behaviors of RC buildings under seismic actions [7]. Beyond deterministic and experimental approaches, uncertainties associated with RC, particularly in seismic regions, have been a crucial research focus [8],[9]. Probabilistic analyses have increasingly been combined with non-linear simulations of RC elements with the aim to consider epistemic and aleatory uncertainties in modeling, seismic inputs, and structural parameters [10]-[12]. For instance, statistical analysis in [13] estimated the probable flexural strength of ductile RC columns by considering uncertainties in materials, sectional properties, and analytical modeling under varying confinement levels. Concerning the concrete beam-column joints equipped with transverse reinforcement, some probabilistic non-linear models have been suggested in [14]. Additionally, [15] examined uncertainties in earthquake characteristics and material properties of concrete and reinforcing steel, while [16] conducted seismic fragility evaluation of RC frames using response surface models calibrated on non-linear Incremental Dynamic Analyses (IDAs) [17] with multiple ground motions. Modern seismic design of RC structures [18]-[20] incorporates overstrength principles based on capacity design [21]. Global structural strength is ensured through ductile failure mechanisms (strong-column weak-beam principle), while member-level ductility is controlled providing a hierarchical order among shear and flexural behaviors. Flexural strengths are typically enhanced via overstrength factors γ_{Rd}, which account for material overstrength variability. However, these factors are primarily calibrated based on reinforcement yield strength and strain hardening [21], often neglecting concrete strength variability, which some studies suggest may lead to non-conservative estimates [22]-[24]. Moreover, research has indicated that existing design codes may not always ensure strong-column weak-beam behavior in RC systems [25]-[27], as plastic rotation of beams and columns, joint locations, and frame height influence structural response.

This study assesses the confinement effects on seismic reliability of new RC frames designed for a high ductility class. A three-storey RC building designed in agreement with seismic design. The site selected is the city of L'Aquila (Italy). After that, an internal RC frame is modelled in the fiber-based software STKO [28] (Scientific ToolKit for Opensees). The confinement model proposed by Mander et al. [29] has been considered. A probabilistic approach both in terms of mechanical properties of materials (steel and concrete) and regarding the seismic input, is adopted. Concerning the materials, the Latin Hypercube Sampling (LHS) technique is selected, with a sample size equal to 30. Regarding the earthquake, a set of 30 natural ground motions scaled according to the seismic hazard of the site is considered. Thereafter, non-linear IDAs [17] are performed, with Interstory Drift Indices (IDIs) as the Engineering Demand Parameters (EDPs) and the spectral acceleration value as Intensity Measure (IM). The seismic hazard curve for the reference site is defined, whereas seismic fragility is analyzed based on appropriate limit state thresholds. Finally, seismic reliability assessment is performed by a convolution integral among seismic hazard curve and seismic fragility curves, and then by applying Poisson's model.

2 SEISMIC DESIGN OF THE CASE STUDY FRAME

A three-storey RC residential building located in the highly seismic area of L'Aquila (Italy) is taken into account. According to the Italian code rules [20], a C25/30 class of concrete and a B450C type of reinforcing steel for the structural elements (columns and beams) are used.

The internal RC frame is represented in Figure 1, which includes the interstorey and the span dimensions. In particular, an interstorey height of 3m, a span length of 5m and an effective area in transverse direction of 5m are considered.

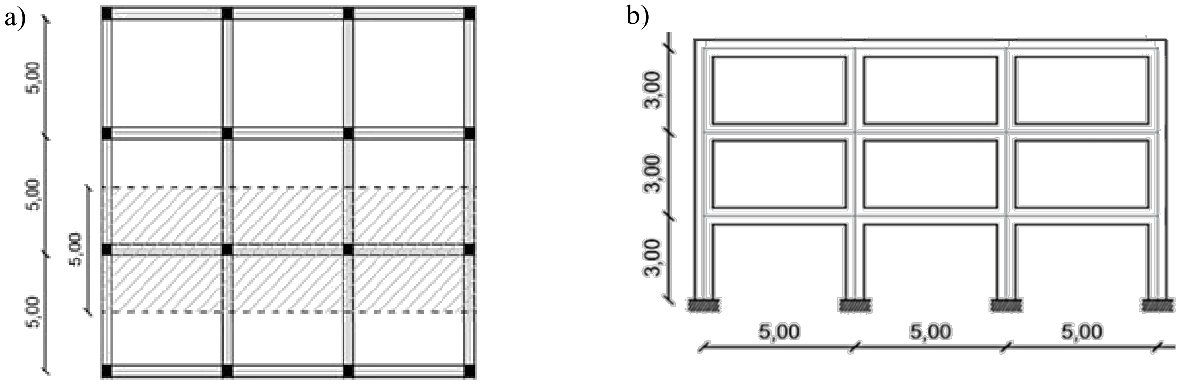

Figure 1. Plan view (a) and front view (b) of the internal RC frame considered. All measurements expressed in meters.

In order to give to the structure a high dissipation capacity, a high ductility class for the internal RC frame is assumed. Concerning the beams, a cross section of width 0.3m and height 0.5m is considered, in which Φ8 vertical stirrups are arranged. The stirrups' spacing in the dissipative zones is 10 cm, while in the non-dissipative they are 15cm spaced. Furthermore, longitudinal bars with diameter Φ18 are arranged, in particular 3Φ18 and 2Φ18 in the upper and lower part of the cross-section of the dissipative are, respectively, arranged. About the columns, a squared cross section with side 0.5m is considered. Stirrups of Φ8 with 10 cm spacing are arranged in the dissipative zones, while in the non-dissipative they are 15cm spaced. Additionally, longitudinal bars with diameter Φ20 are arranged, the disposal is symmetric in the two directions. A clear concrete cover of 3cm for all beams and columns is adopted.

3 MODELLING, MATERIALS SAMPLING AND INCREMENTAL DYNAMIC ANALYSES (IDAS)

The internal RC frame is implemented in the fiber-based software STKO [28] (Scientific ToolKit for Opensees), a graphical interface used as support for the Opensees software. Fiber modeling involves discretizing the cross-section into a certain number of fibers, each assigned the constitutive relationships of the selected materials. This approach allows for the consideration of nonlinearities through the material constitutive laws. In this case study, a non-linear modelling regime is adopted for concrete; for this purpose, the model "*Concrete02*" is considered. In relation to the confined concrete core, the confinement model proposed by Mander et al. [29] is adopted. Concerning the reinforcing bars, the "*ReinforcingSteel*" model is adopted, as it accounts for buckling and fatigue failure phenomena. Moreover, in order to take into account the aleatory nature of both seismic inputs and materials, a probabilistic approach is used. To achieve this, a set of 30 natural ground motions scaled according to the seismic hazard of the site is considered, meanwhile for the uncertainties of both steel and concrete a sampling of their mechanical properties is performed. The sampled parameters are four for steel (i.e., ultimate and yielding strength, elastic modulus, ultimate strain) and one for concrete (compressive strength) respectively. The Latin Hypercube Sampling (LHS) technique is the method selected, with a sample size equal to 30.

To carry out IDAs [17], two quantities need to be defined: the IM and EDPs. The spectral acceleration value $S_a(T)$ as IM is selected for this case study. In particular, 10 values considered in the range [0.1g – 1g] with a step of 0.1. According to the local seismic hazard, the spectral acceleration value in correspondence of the first period of the structure at Near Collapse Limit State is equal to 0.87g ($S_a(T_1)$ = 0.87g). Based on this value, the upper end of the selected range is equal to 1g. The Interstorey Drift Index peak values of each floor of the structure ($IDIs_{,peak}$) are selected as EDPs in this case study. For a given value of IM, a set of 900 numerical analyses is performed (30 sampling x 30 seismic inputs). Hence, a total number of 9000 non-linear time history is carried out. Since it is assumed that the EDPs follow a lognormal distribution [31]-[34], the parameters that characterize the distribution, such as the mean and the standard deviation, are computed. Moreover, three different percentile levels [35]-[40] are considered (i.e., 16% - 50% - 84%). Regarding the cases of collapse, both those of the flexural type and those due to failure to fulfill the shear verification are considered. The cases of collapse previously mentioned are not taken into account in the computation of statistics parameters of the IDAs. In Figure 2, the IDA curves obtained are represented. In detail, the interstorey drift index peak values ($IDI_{,1,peak}$ $IDI_{,2\ peak}$, $IDI_{,3\ peak}$) and the maximum value among the three ($IDI_{,max,\ peak}$) depending on the intensity measures are depicted. It can be seen that increasing the IM values, the dispersion is higher; this happens because, for higher IM levels, the uncertainties related to the seismic events and sampling have a greater impact. Furthermore, it is noticeable that the IDI values obtained for the third floor of the structure (Figure 2(c)) are smaller than on the other two floors.

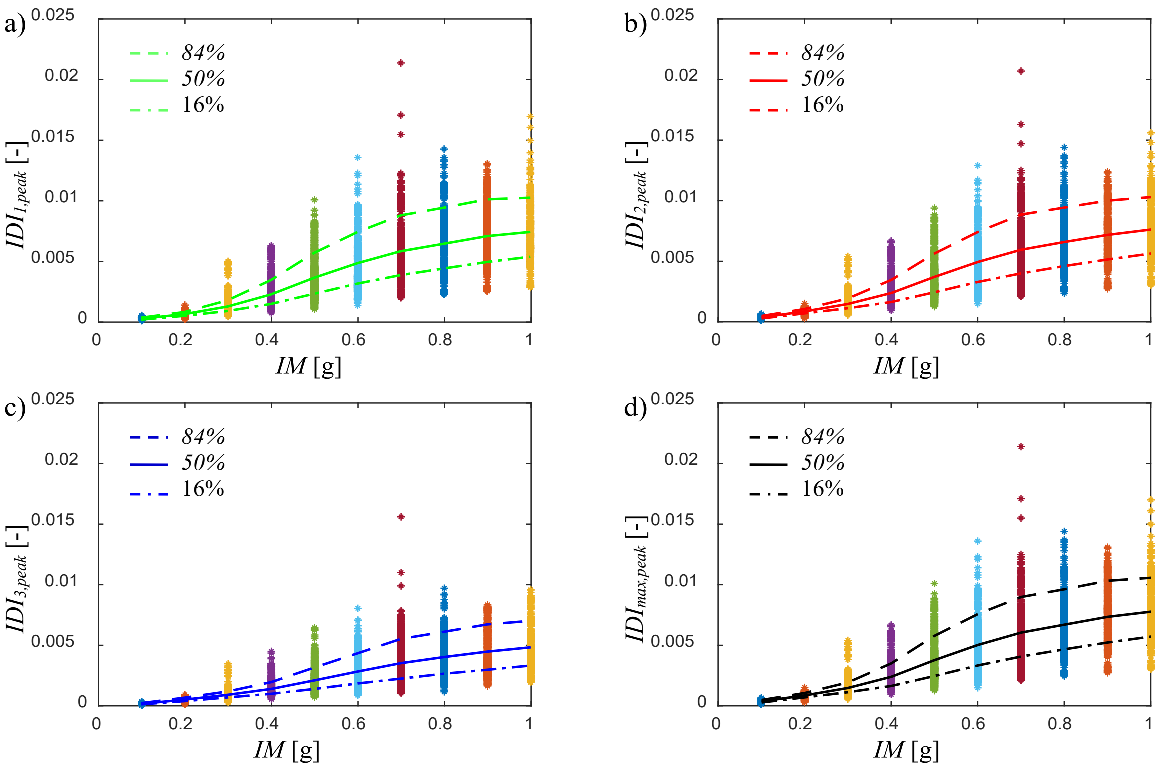

Figure 2. IDAs curves at the 16%, 50% and 84% percentiles. The curves relating to the first floor (a), second floor (b), third floor (c) and the maximum value among the three (d) are shown.

4 SEISMIC HAZARD CURVE DEFINITION

In order to delineate the seismic hazard curve, the recommendation of the Italian codes [20] and the data provided by the INGV [30] for the reference site of L'Aquila are observed. The type of soil considered belongs to category B, with a horizontal topographic surface, while the service life adopted is equal to 50 years. The seismic hazard curve obtained is represented in Figure 4. The graphic presents a semi-logarithmic scale, and the mean annual rate of exceedance (λ_c) depending on several IM values is illustrated.

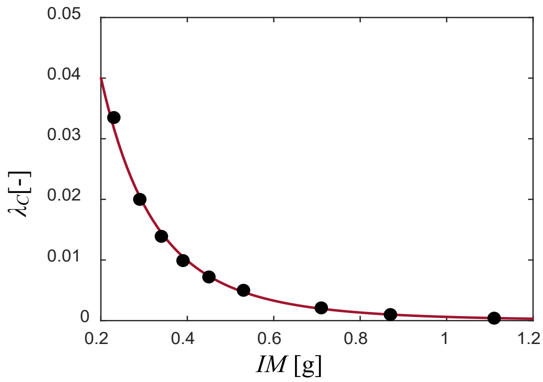

Figure 3. Seismic hazard curve for L'Aquila.

5 FRAGILITY CURVES DEVELOPMENT

Seismic fragility must be evaluated to perform the reliability analysis. Seismic fragility is defined as the probability that a structural system will exceed specified limit state thresholds for a given IM value. Limit State thresholds for this study are expressed in terms of interstorey drift index (IDI_{LS}), the values adopted are taken from SEAOC [41]; four limit states are considered: Fully Operational (FO), Operational (O), Life Safety (LS) and Near Collapse (NC). The IDI_{LS} values are shown in Table 1.

Performance Level	Limit State	IDI_{LS}(%)
FO	LS1	0.3
O	LS2	0.6
LS	LS3	1.5
NC	LS4	2.5

Table 1: Limit state threshold values considered.

In order to obtain the fragility curves, the total probability theorem is used. In Figure 4, the fragility curves are shown, in terms of the probability of exceedance (P_f) related to the IDI_{Peak} of each floor depending on the range of IM values adopted for the four limit states. It is important to highlight that for the lowest limit state (i.e., the first two), the threshold value of the probability of exceedance at lower intensity measures levels is attained. Furthermore, higher values of exceedance probability for the Fully Operational and Operational limit state on the first and second floor than those for the third floor are obtained, coherently with the results shown in terms of IDAs.

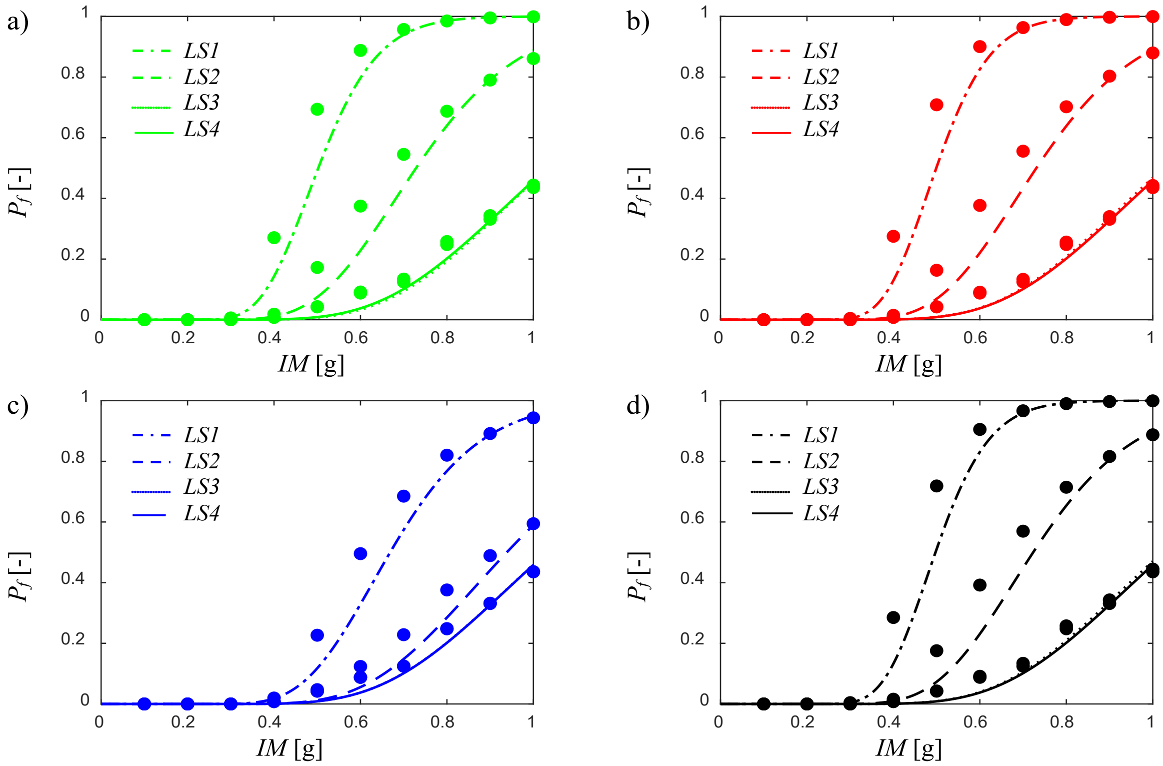

Figure 4. Fragility curves for the four limit states considered. The curves related to the first floor (a), second floor (b), third floor (c) and the maximum value among the three (d) are shown.

6 SEISMIC RELIABILITY ANALYSES

After defining the seismic hazard curve for the reference site (L'Aquila) and obtaining the seismic fragility curves for the case under study, the seismic reliability curves can be determined by comparing the Performance Objective curve (PO) to the Structural Performance curves (SPs). With respect to the PO curve, the limit states Fully Operational (FO) - Operational (O) – Life Safety (LS) – Near Collapse (NC) are considered, with the corresponding values of exceedance probability selected in accordance with the FEMA [42] guidelines. The values adopted are shown in Table 2. It is important to highlight that as the severity of the limit state increases, the corresponding limit value becomes more stringent.

Performance Level	Limit State	P_f [50 years]
FO	LS1	5.00E-01
O	LS2	1.60E-01
LS	LS3	2.20E-02
NC	LS4	1.50E-03

Table 2: Target failure probabilities [42].

To evaluate seismic reliability, a convolution integral among seismic hazard curve and seismic fragility curves is performed. In this manner, the mean annual exceedance rate is obtained. Given that a reference service life of 50 years (V_R = 50 years) is adopted, the previously obtained exceedance rate must be distributed over this time period. To do this, the Poissons's model is adopted. In Figure 5, the seismic reliability curves obtained are represented. It is noteworthy that the P_f values obtained fulfill the P_f limit values concerning the LS1-

LS2 for all the three floors of the structure respectively. The P_f limit value of the LS3 is slightly violated, whereas the P_f limit value of the LS4 (i.e. the most severe) is always exceeded. Furthermore, the P_f values obtained for the third floor are lower than those obtained for the other two ones.

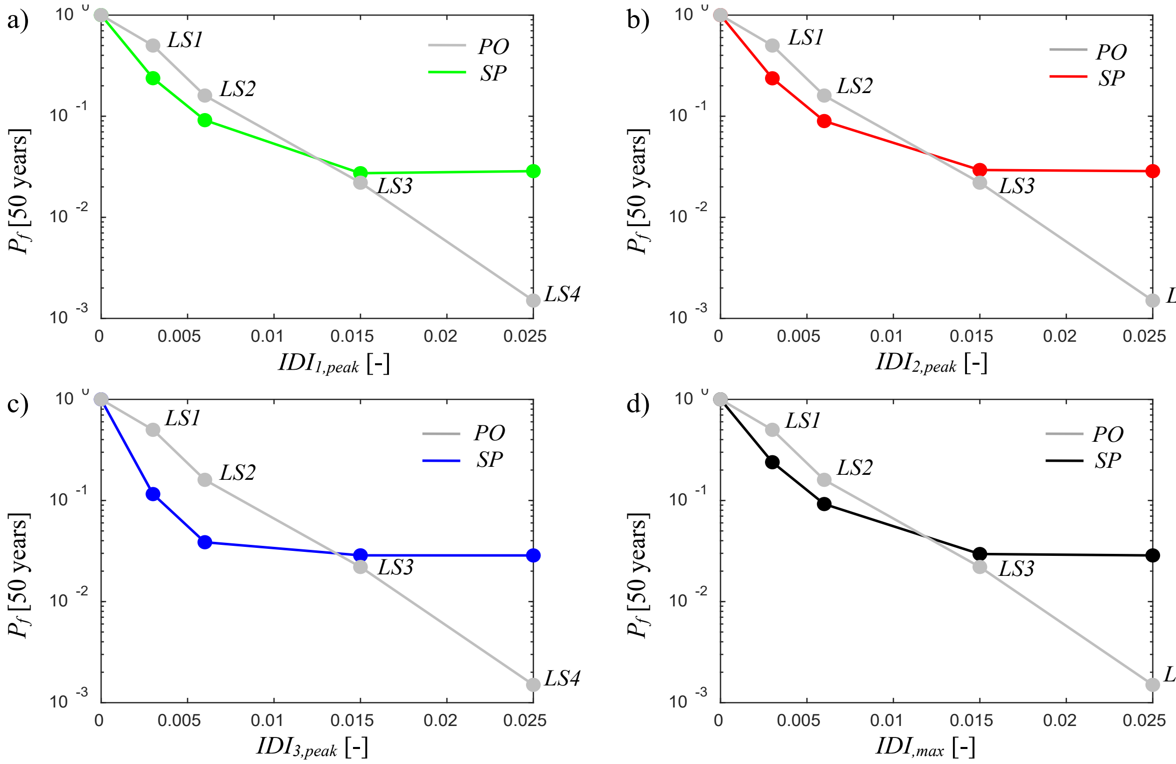

Figure 5. Comparison among the reliability curve of the first floor (a), second floor (b), third floor (c) and of the maximum value among the three (d) with the "performance objective" curve (grey) for the four limit states considered.

7 CONCLUSIONS

In this work, the influence of concrete confinement on the seismic reliability of RC frames has been studied. The first step was the seismic design of a three-storey RC building located in the highly seismic area of L'Aquila (Italy). After that, an internal RC frame has been modelled in the fiber-based software in order to perform non-linear time history analyses. To account for uncertainties due to the randomness of the earthquake, a set of 30 natural ground motions was selected and scaled with respect to the site's seismic hazard. Furthermore, mechanical properties of both steel and concrete are sampled to take into account their uncertainties. Defined the interstorey drift index peak values of each floor as EDPs and the spectral acceleration value as IM, IDAs are performed. A lognormal distribution for the engineering demand parameters is assumed, allowing the evaluation at different percentile values (i.e., 16% - 50% - 84%). The IDAs curves showed a greater dispersion at higher IMs levels, this happens because as the severity of the IMs increases, the weight of the uncertainties related to both the earthquake and materials increases. After that, fragility curves are obtained assuming limit state thresholds values in terms of interstory drift indices. Lastly, seismic reliability is assessed through a convolution integral among seismic hazard curve and seismic fragility curves, by applying Poisson's model to determine the probability of exceedance over the 50-year reference lifetime. The results have shown that the lowest limit states (FO – O) are completely respected, the third limit state (LS) is slightly violated, and the last (i.e. the most severe) is always exceeded.

ACKNOWLEDGMENTS

This work was carried out within the RETURN Extended Partnership and received funding from the European Union Next-GenerationEU (National Recovery and Resilience Plan—NRRP, Mission 4, Component 2, Investment 1.3—D.D. 1243 2/8/2022, PE0000005).

This work is also part of the collaborative activity developed by the authors within the framework of the WP 11 – Task 11.3 – ReLUIS.

REFERENCES

[1] M. De Iuliis, P. Castaldo, B. Palazzo, Seismic demand analysis of inelastic SDOF systems designed according to the NTC 2008 for L'Aquila earthquake | Analisi della domanda sismica inelastica del terremoto de L'Aquila su sistemi dimensionati secondo le NTC 2008. *Ingegneria Sismica*, **27**(3), 55-68, 2010.

[2] M. De Iuliis, C. Faella, Effectiveness analysis of a semiactive base isolation strategy using information from an early-warning network. *Engineering Structures*, **52**, 518-535, 2013.

[3] P. Castaldo, B. Palazzo, T. Ferrentino, Seismic reliability-based ductility demand evaluation for inelastic base-isolated structures with friction pendulum devices, *Earthquake Engineering and Structural Dynamics*, **46**, 1245–1266, 2017.

[4] M. De Iuliis, E. Miceli, P. Castaldo, Machine learning modelling of structural re-sponse for different seismic signal characteristics: A parametric analysis. *Applied Soft Computing*, **164**, 112026, 2024.

[5] M. De Iuliis, E. Miceli, P. Castaldo, An energy framework to control viscoelastic semi-active devices in plan-wise one-way asymmetric systems, *Structural Control and Health Monitoring*, 2025, 10.1155/stc/7091316.

[6] L. Petti, M. De Iuliis, Robust design of a single tuned mass damper for controlling torsional response of asymmetric-plan systems. *Journal of Earthquake Engineering*, **13**(1), 108-128, 2009.

[7] M. Polese, G.M. Verderame, C. Mariniello, I. Iervolino, G. Manfredi, Vulnerability curves for gravity load designed RC buildings in Naples – Italy. *Journal of Earthquake Engineering*, **12**(S2), 234-245, 2008.

[8] E. Miceli, D. Gino, P. Castaldo, Approaches to estimate global safety factors for reliability assessment of RC structures using non-linear numerical analyses. *Engineering Structures*, **311**, 118193, 2024.

[9] P. Castaldo, D. Gino, G. Bertagnoli, G. Mancini, Resistance model uncertainty in non-linear finite element analyses of cyclically loaded reinforced concrete systems, *Engineering Structures*, **211**, 110496, 2020.

[10] G. Bertagnoli, M. Ferrara, E. Miceli, P. Castaldo, L. Giordano, Safety assessment of an existing bridge deck subject to different damage scenarios through the global safety format ECOV. *Engineering Structures*, **306**, 117859, 2024.

[11] M. Ferrara, D. Gino, E. Miceli, L. Giordano, M. Malavisi, G. Bertagnoli, Safety assessment of existing prestressed reinforced concrete bridge decks through different approaches, *Structural Concrete*, **25**(3), 1637-1657, 2024.

[12] D. Gino, E. Miceli, P. Castaldo, A. Recupero, G. Mancini, Strain-based method for assessment of global resistance safety factors for NLNAs of reinforced concrete structures. *Engineering Structures*, **304**, 117625, 2024.

[13] C. Aydemir, M. Zorbozan, Uncertainty Analysis of Flexural Overstrength Ratio for RC Columns. *Journal of structural engineering* **138**(8), 1042-1053, 2012.

[14] W.M. Hassan, M. Elmorsy, Probabilistic Beam–Column Joint Model for Seismic Analysis of Concrete Frames. *Journal of Structural Engineering,* **148**(4), 04022011, 1-19, 2022.

[15] C.L. Segura, S. Sattar, Uncertainty in the Seismic response of Reinforced Concrete structures due to material variability. *17th World Conference on Earthquake Engineering, 17WCEE*, Sendai, Japan, September 13-18, 2020.

[16] N. Buratti, B. Ferracuti, M. Savoia, Response Surface with random factors for seismic fragility of reinforced concrete frames, *Structural Safety* **32**, 42-51, 2010.

[17] D. Vamvatsikos and C.A. Cornell, *Incremental Dynamic Analysis, Department of Civil and Environmental Engineering*. Stanford University, 2002.

[18] European Standards, *Eurocode 2, Design of concrete structures - Part 1-1: General rules and rules for buildings*. Brussels, Belgium, 2004.

[19] European Standards, *Eurocode 8, Design of structures for earthquake resistance - Part 1: General rules - seismic actions and rules for buildings*. Brussels, Belgium, 1998.

[20] Ministry of Infrastructure and Transportation, *Italian Technical Standards for Construction*, Rome, Italy, 2018).

[21] T. Paulay, M.J.N. Priestley, *Seismic design of reinforced concrete and masonry buildings*. Wiley, New York, 1992.

[22] C. Galasso, G. Maddaloni, E. Cosenza, Uncertainly Analysis of Flexural Overstrength for Capacity Design of RC Beams. *Journal of structural engineering*, **140**(7), 2014.

[23] E. Miceli, P. Castaldo, Robustness improvements for 2D reinforced concrete moment resisting frames: Parametric study by means of NLFE analyses. *Structural Concrete*, **25**(1), 9-31, 2024.

[24] E. Miceli, S. Ferrara, P. Castaldo, Confinement effects within the seismic design of reinforced concrete frames: reliability assessment and comparison. *Engineering Structures*, **313**, 118248, 2024.

[25] I.K. Sudarsana, I.A.M. Budiwati, P.W. Aditya, Effect of column to beam strength ratio on performance of reinforced concrete frames. *Proceedings Of the 1st International Conference On Engineering Technology And Industrial Application*, Surakarta, Indonesia, 2014.

[26] M. Ghorbanzadeh, F. Khoshnoudian, The effect of strong column-weak beam ratio on the collapse behaviour of reinforced concrete moment frames subjected to near-field earthquakes, *Journal of Earthquake Engineering*, 26(**8**), 4030-4053, 2020.

[27] Kim, C.-S. et al. (2022) Column-to-beam flexural strength ratio for performance-based design of RC moment frames. *Journal of Building Engineering* 46103645.

[28] M. Petracca, F. Candeloro, G. Camata, *STKO user manual ASDEA Software*, 2021.

[29] J.B. Mander, M.J.N. Priestley, R. Park, Theoretical Stress-Strain Model for Confined Concrete. *Journal of Structural Engineering*, **114**(8), 1804-1826, 1988.

[30] National Institute of Geophysics and Volcanology (INGV), *Annex A and B to the Technical Standards for Construction: Seismic hazard*, 2008.

[31] P. Castaldo, G. Amendola, L. Giordano, E. Miceli, Seismic Reliability Assessment Of Isolated Multi-Span Continuous Deck Bridges. *Ingegneria Sismica*, **39**(3), 26-51, 2022.

[32] E. Miceli, D. Gino, P. Castaldo, Reliability Assessment Of Robustness For Reinforced Concrete Moment Resisting Frames, Developments in the Built Environment, 2025, 100639, https://doi.org/10.1016/j.dibe.2025.100639.

[33] D. Gino, E. Miceli, L. Giordano, G.C. Marano, P. Castaldo, Influence of Masonry Infills on Seismic Performance of an Existing RC Building Retrofitted by Means of FPS Devices. *Applied Sciences (Switzerland)*, **13**(6), 3509, 2023.

[34] P. Castaldo, E. Miceli, Optimal single concave sliding device properties for isolated multi-span continuous deck bridges depending on the ground motion characteristics. *Soil Dynamics and Earthquake Engineering*, **173**, 108128, 2023.

[35] R. Troisi, S. De Simone, M. Franco, Illegal firm behaviour and environmental hazard: The case of waste disposal. *European Management Review*, **21**(3), 605-617, 2024.

[36] R. Troisi, G. Alfano, Is "justice hurried actually justice buried"? An organisational perspective of the Italian criminal justice. *International Journal of Public Sector Management*, **36**(1), 94-109, 2023.

[37] A. Nese, R. Troisi, Individual Preferences and Job Characteristics: An Analysis of Cooperative Credit Banks, *Labour*, **28**(2), 233–249, 2014.

[38] R. Troisi, S. De Simone, M. Franco, The resilience of the regional ecosystems: Healthcare-service organizations, public agents and communities in times of Covid-19. *Mecosan*, (125), 83-97, 2023.

[39] R. Troisi, A. Nese, R. Blanco-Gregory, M.A. Giovanniello, The Effects of Corruption and Innovation on Sustainability: A Firm-Level Analysis. *Sustainability (Switzerland)*, **15**(3), 1848, 2023.

[40] M. Musella, R. Troisi, Property rights and incentives in social cooperatives, *AIEL Series in Labour Economics*, **4**, 47-61, 2009.

[41] SEAOC Vision 2000 Committee, *Performance-based seismic engineering*. California, Sacramento, CA, 1995.

[42] Building seismic safety council, *FEMA 274: NEHRP Commentary on the Guidelines for the Seismic Rehabilitation of Buildings*. Washington, D.C, 1994.